2.5D Acoustic Finite-Difference Modeling in variable density media

J. Costa, A. Novais, F. de Assis Silva Neto, and M. Tygel

email: *jesse@ufpa.br*

keywords: *Modeling, acoustic, finite-difference*

ABSTRACT

Numerical solutions of the acoustic wave equation in media where the physical properties depend only on two of the spatial coordinates, can be obtained by multiple application of 2D finite-difference (FD) schemes. This 2.5D approach presents a smaller computation cost than the solution of the corresponding 3D problem. This work extends previous formulations of numerical 2.5D solutions of the acoustic wave equation with constant density to variable-density media. The acoustic wave equation is formulated as a system of partial differential equations for the wavefields of pressure and particle velocity in isotropic, arbitrarily inhomogeneous media. Absorbing boundary conditions for perfect impedance match are formulated for the 2.5D case. A comparison of the stability conditions for the 2.5D and 3D finite-difference schemes of arbitrary order leads to a maximum-wavenumber condition for the inverse Fourier transform. A discussion of the numerical dispersion and numerical anisotropy relations shows that these effects increase with decreasing wavenumbers in the out-of-plane direction. The quality of the numerical solution is confirmed by a comparison to the analytic solution for a homogeneous medium. As a quality control in inhomogeneous media, a comparison of the 2.5D results to corresponding 3D FD results for the Marmousi model shows good agreement.

INTRODUCTION

Modeling of seismic wavefields in three dimensions is a very desirable task to understand their properties. However, 3D modeling is very expensive and requires extensive computational resources, even for a modest-sized model. Therefore, up to now it has been mainly performed using supercomputers.

If the modeling of 3D wave propagation is carried out in media with only 2D variations of the acoustic properties, the seismic line being positioned within the symmetry plane, this is generally referred to as the 2.5D situation. This situation is very interesting from the perspective of numerical experiments as the medium symmetry can be used to reduce the complexity of the numerical task.

The modeling of seismic wave propagation in the 2.5D situation is helpful to approximately simulate situations where sources and receivers are located within the same plane. Some of the more common applications are conventional 2D seismic surveys, i.e., where the sources and receivers follow a single seismic line (Liner, 1991), and seismic borehole tomography (Williamson and Pratt, 1995).

In his 1991 paper, Liner postulated the existence of a 2.5D wave equation the solution of which would provide 3D waves within the symmetry plane from only in-plane calculations. His equation, however, is only exact for constant velocity. Based on a Fourier transform in the out-of-plane direction, Song and Williamson (1995) presented an approach by repeated 2D finite-difference modeling in the frequency domain to find the exact solution of the 3D wave equation in the 2.5D situation for acoustic media with constant density, and applied their results to tomographic problems. They proved the quality of their results by a comparison to 3D modeling with the Born approximation. Cao and Greenhalgh (1998) and Zhou and Greenhalgh (1998) determined the stability and absorbing boundary conditions for this 2.5D FD approach, again for constant density, and compared the implementations in the time and frequency domains. In these papers, the inverse Fourier transform is carried out by a sum up to the Nyquist wavenumber. Re-

cently, Novais and Santos (2004) revisited this approach and obtained a maximum wavenumber criterion and sampling limits in the time domain from a comparison of the 2.5D and 3D stability conditions.

In this work, we extend the time domain version of Novais and Santos (2004) to media with variable density. Moreover, we generalize the method to the computation of the complete acoustic wavefield, composed of the three components of the particle velocity and the pressure field. We present the stability conditions for the corresponding higher-order finite-difference schemes and validate them for one of these schemes in homogeneous media. Finally, we validate the 2.5D algorithm against 3D finite-difference modeling for a simple inhomogeneous model and the Marmousi model.

2.5D MODELING

The complete acoustic wavefield in an arbitrary 3D acoustic medium is governed by the equation system (Aki and Richards, 1980)

$$\partial_t v_j(\mathbf{x},t) = -\frac{1}{\rho(\mathbf{x})}\partial_j P(\mathbf{x},t) + \frac{1}{\rho(\mathbf{x})} f_j(\mathbf{x},t)\,, \tag{1}$$

$$\partial_t P(\mathbf{x},t) = -\rho(\mathbf{x})c^2(\mathbf{x})\partial_j v_j(\mathbf{x},t) + q(\mathbf{x},t)\,, \tag{2}$$

where $v_j(\mathbf{x},t)$ is the particle velocity in position $\mathbf{x}$ and instant t, $P(\mathbf{x},t)$ is the pressure field, $\rho(\mathbf{x})$ is the density and $c(\mathbf{x})$ is the propagation velocity in the medium.

In 2.5D modeling, it is supposed that the physical properties of the medium are invariant under translations in one direction. In this work this direction is, as usual, described by the coordinate x_2. Moreover, sources and receivers are considered be located in plane $x_2 = 0$. Applying the Fourier transform in this coordinate to the above equation system, we obtain

$$\begin{aligned}
\partial_t v_J &= -\frac{1}{\rho(\mathbf{X})}\partial_J P + \frac{f_J(t)\delta(\mathbf{X}-\mathbf{X}_s)}{\rho(\mathbf{X})}\,,\\
\partial_t v_2 &= -\frac{1}{\rho(\mathbf{X})} ik_2 P + \frac{f_2(t)}{\rho(\mathbf{X})}\,,\\
\partial_t P &= -\rho(\mathbf{X})c^2(\mathbf{X})(\partial_J v_J + ik_2 v_2) + q(t)\delta(\mathbf{X}-\mathbf{X}_s)\,,
\end{aligned}$$

where k_2 is wavenumber associated with the coordinate x_2. All fields in the above equation system are functions of $(\mathbf{X}, k_2, t)$, with $\mathbf{X} = (x_1, x_3)$, and $\mathbf{X}_s$ is the source location. We have adopted the sum convention, where the subscript J assumes the values 1 and 3. Since we are interested in the wave field in the x_1x_3-plane, the bipolar source has no component f_2. In this case, the component $v_2(\mathbf{x},t)$ is an odd function in coordinate x_2, thus its Fourier transform $v_2(\mathbf{X},k_2,t)$ is purely imaginary. By defining the real field $u_2(\mathbf{X},k_2,t) \equiv iv_2(\mathbf{X},k_2,t)$, we can write the system to be computed by finite differences as

$$\begin{aligned}
\partial_t v_J &= -\frac{1}{\rho(\mathbf{X})}\partial_J P + \frac{f_J(t)\delta(\mathbf{X}-\mathbf{X}_s)}{\rho(\mathbf{X})}\,,\\
\partial_t u_2 &= \frac{1}{\rho(\mathbf{X})} k_2 P\,,\\
\partial_t P &= -\rho(\mathbf{X})c^2(\mathbf{X})(\partial_J v_J + k_2 u_2) + q(t)\delta(\mathbf{X}-\mathbf{X}_s)\,.
\end{aligned} \tag{3}$$

The finite-difference method consists in sampling the wavefield and the physical properties of the medium on a regular grid and in approximating the differential operator by a difference operator defined on the grid. We use a staggered grid in space and in time. The components of the particle velocity field, v_j, and the values of the pressure field, P, are sampled at different grid nodes (Levander, 1988), as indicated

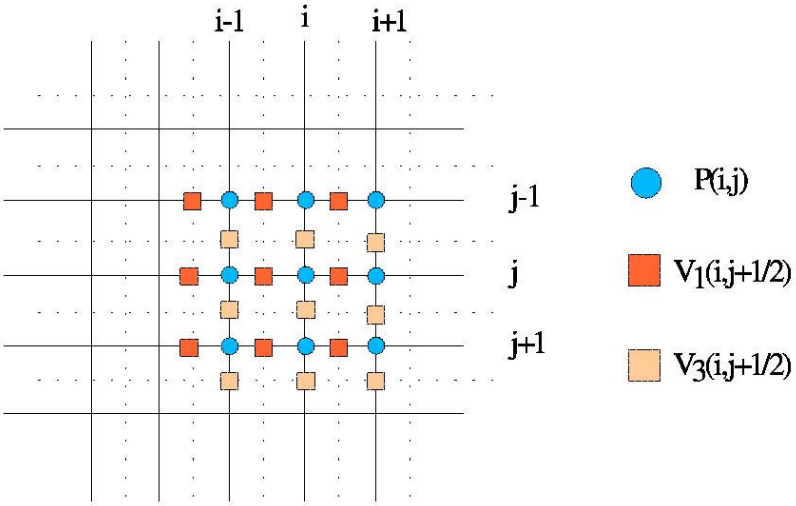

Figure 1: Grid used for the finite-difference scheme. The sampling of the velocity and pressure fields on a staggered grid reduces the local error.

in Figure 1. The approximation of the above equations on the grid yields the difference scheme

$$\begin{aligned}
\mathbf{D}_t^+ {v_1}_{j+\frac{1}{2},k}^{n-\frac{1}{2}} &= \frac{1}{\rho_{j+\frac{1}{2},k}} \left(\mathbf{D}_1^+ P_{j,k}^n + {f_1}_{j+\frac{1}{2},k}^{n+\frac{1}{2}} \right) \\
\mathbf{D}_t^+ {v_3}_{j,k+\frac{1}{2}}^{n-\frac{1}{2}} &= \frac{1}{\rho_{j,k+\frac{1}{2}}} \left(\mathbf{D}_3^+ P_{j,k}^n + {f_3}_{j,k+\frac{1}{2}}^{n+\frac{1}{2}} \right) \\
\mathbf{D}_t^+ {u_2}_{j,k}^{n-\frac{1}{2}} &= -k_2 \, P_{j,k}^n \\
\mathbf{D}_t^- P_{j,k}^{n+1} &= K_{j,k} \left(\mathbf{D}_1^- {v_1}_{j+\frac{1}{2},k}^{n+\frac{1}{2}} + \mathbf{D}_3^- {v_3}_{j,k+\frac{1}{2}}^{n-\frac{1}{2}} + k_2 \, {u_2}_{j,k}^{n+\frac{1}{2}} \right) + q_{j,k}^{n+\frac{1}{2}} \, .
\end{aligned}$$

The pressure field is sampled at the grid positions $x_1 = j\Delta x$, $x_3 = k\Delta x$ and instants $t = n\Delta t$; the velocity field is sampled in intermediate grid positions as displayed in Figure 1 and at the instants $t = (n + \frac{1}{2})\Delta t$. Here, Δx and Δt are the spatial and temporal sampling intervals, respectively. The notations $\mathbf{D}^+$ e $\mathbf{D}^-$ indicate forward and backward finite-difference operators (Iserles, 1996), respectively, and $K_{j,k} = \rho_{j,k} c_{j,k}^2$.

The discretization interval of the wavenumber is $\Delta k_2 = \pi/(\Delta x \, \max(N_1, N_3))$, where N_1 and N_3 indicate the number of samples in directions x_1 and x_3, respectively. After the velocity and pressure fields are calculated in the wavenumber domain for all values of the wavenumber k_2, the acoustic fields at the receiver (with $x_2 = 0$) is obtained by applying the inverse Fourier transform, which in this case reduces to a simple sum over all wavenumbers, i.e.,

$$\begin{aligned}
v_I(x_1, x_2 = 0, x_3, t) &= \frac{\Delta k_2}{\pi} \sum_{k_2} v_I(x_1, k_2, x_3, t) \, , \\
P(x_1, x_2 = 0, x_3, t) &= \frac{\Delta k_2}{\pi} \sum_{k_2} P(x_1, k_2, x_3, t) \, ,
\end{aligned}$$

because all functions are even in coordinate x_2.

STABILITY

The stability of a finite-difference scheme is evaluated using the von Neumann criterion (Thomas, 1995). The convolutional difference operators, $\mathbf{D}_1^{\pm}$ and $\mathbf{D}_3^{\pm}$, are of order $2N$, and have the form

$$\begin{aligned} \mathbf{D}^{+} f_i &= \frac{1}{\Delta x} \sum_{j=-N+1}^{N} d_j^{(1)} f_{i-j} \,, \\ \mathbf{D}^{-} f_i &= \frac{1}{\Delta x} \sum_{j=-N}^{N-1} d_j^{(1)} f_{i-j} \,. \end{aligned}$$

where the $d_j^{(1)}$ are the operator coefficients. In this notation, the coefficients of the corresponding central difference operator for the second derivative of the same order $2N$ are determined by the convolution

$$d_i^{(2)} = \frac{1}{(\Delta x)^2} \sum_{j=-N+1}^{N} d_j^{(1)} d_{i-j}^{(1)} \,, \qquad i = 2N-1, ..., 2N-1 \quad .$$

After replacing the acoustic field by that of a plane wave in the difference equations, the condition for a nontrivial solution of the scheme to exist can be written in the form

$$\sin^2\left(\frac{\omega \Delta t}{2}\right) = \left(\frac{c\Delta t}{\Delta x}\right)^2 \left[\left(\frac{k_2 \Delta x}{2}\right)^2 + \sum_{j=1}^{2N-1} d_j^{(2)} \left(\sin^2 \frac{j k_1 \Delta x}{2} + \sin^2 \frac{j k_3 \Delta x}{2}\right)\right] \,, \qquad (4)$$

where ω is angular frequency and (k_1, k_2, k_3) is the wavenumber vector. To guarantee the stability of the FD scheme, the right side of equation (4) must be less or equal to 1. Thus,

$$\frac{c\Delta t}{\Delta x} \leq \frac{1}{\sqrt{\left(\frac{k_2 \Delta x}{2}\right)^2 + |d_0^{(2)}|}} \,, \qquad (5)$$

where we have used that the derivate operator applied a constant function has to yield zero, which implies $d_0^{(2)} - 2\sum_{j=1}^{2N-1} d_j^{(2)} = 0$. Inequality (5) defines the CFL condition, since its left side is the Courant number, $\mu = c\Delta t/\Delta x$ (Thomas, 1995). Similarly, the stability condition for the corresponding 3D finite-difference scheme is

$$\frac{c\Delta t}{\Delta x} \leq \sqrt{\frac{2}{3|d_0^{(2)}|}} \,. \qquad (6)$$

If we require the 2.5D scheme to satisfy the relation (6) up to the maximum value of k_2, we obtain the condition

$$k_{2\max} \leq \frac{\sqrt{2|d_0^{(2)}|}}{\Delta x} \,. \qquad (7)$$

Utilizing equation (4), we can evaluate the behaviour of the FD scheme with respect to numerical dispersion and anisotropy. For example, Figure 2 shows the curves of numerical dispersion of a 2.5D FD scheme of order 12, for different directions of the wavenumber vector.

For $k_2 = 0$, the 2.5D FD scheme coincides with the corresponding 2D scheme. In this case, we observe that the scheme suffers from almost no dispersion or numerical anisotropy, if we choose $\Delta x \leq \lambda_{\min}/3$, where $\lambda_{\min}$ is the minimum wave length involved in the propagation. This result shows that higher order finite-difference schemes reduce the dispersion and numerical anisotropy. On the other hand, for $k_2 = k_{2\max}$, the 2.5D FD dispersion relation follows closely the exact one, thus not introducing any additional numerical dispersion or anisotropy.

In this work, we use a second-order difference operator for the time derivative, $\mathbf{D}_t$, and the space derivatives, $\mathbf{D}_1$ and $\mathbf{D}_3$, are approximated by a 12th-order finite-difference operator, with the purpose of reducing the spatial sampling interval and thus of guaranteeing a higher numerical precision. The operator coefficients are calculated applying the auto-similarity criterion described by Karrenbach (1995).

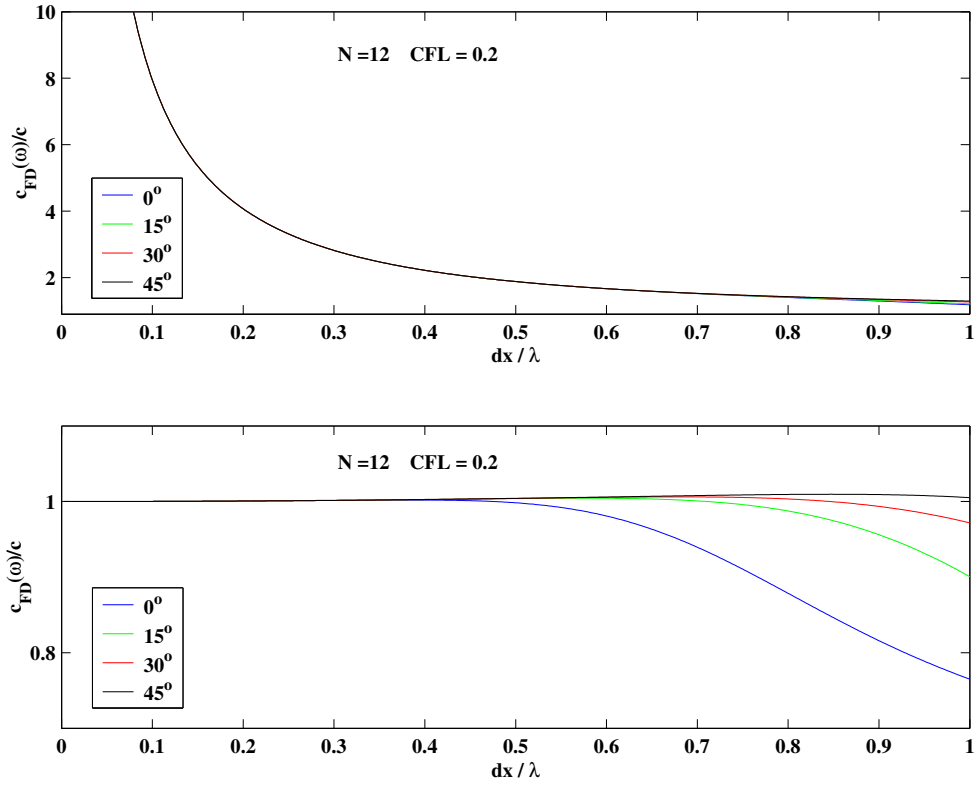

Figure 2: Normalized phase velocity $c_{FD}(\omega)/c$ for different propagation directions as a function of the ratio $\Delta x/\lambda$, where λ is the wavelength. The finite-difference scheme is of 12th order. The CFL number is 0.20. Top: For $k_2 = k_{2\max}$, both the 2.5D exact dispersion relation and its FD approximation show strong dispersion for small wavenumber components of the wavefield. These curves also show the FD scheme does not present considerable numerical anisotropy for large k_2 values. Bottom: For $k_2 = 0$, this FD scheme does produce nonnegligible numerical dispersion and numerical anisotropy if Δx exceeds $\lambda/3$.

VALIDATION

The implementation of a 2.5D scheme requires little change in the corresponding 2D finite-difference scheme. We base our 2.5D scheme on the 2D scheme presented by Neto and Costa (2004). The free surface and absorbing boundary conditions are direct adaptions from the 2D case. In this section, we compare the results of the proposed scheme with the analytic solution for the field pressure in a homogeneous medium

$$P(\mathbf{x}, t; \mathbf{x}_s) = \frac{1}{4\pi\|\mathbf{x} - \mathbf{x}_s\|} w\left(t - \frac{\|\mathbf{x} - \mathbf{x}\|}{c}\right) ,$$

where $\mathbf{x}_s$ is the source location and $w(t)$ is the source pulse.

To test the algorithm, we have applied it to a homogeneous medium with wave velocity of 3000 m/s. The receiver was positioned at a distance of 1500 m from the source and the source pulse was the derivative of a Ricker wavelet with a dominant frequency of 15 Hz. The spatial sampling interval was $\Delta x = 12$ m, and the receiver signal was sampled at every 2 ms. Figure 3 shows that the 2.5D FD trace agrees fairly well with the analytic one. The maximum error is of the order of 5%.

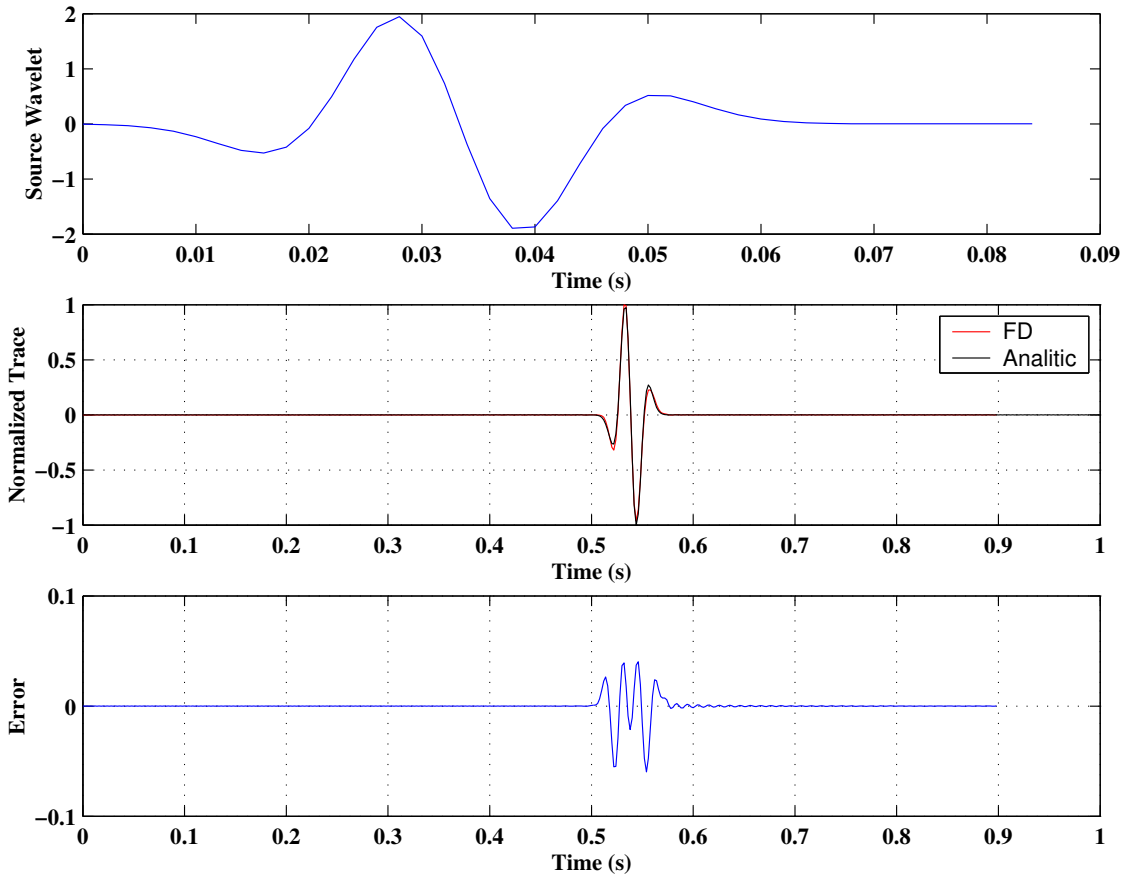

Figure 3: Comparison of the 2.5D finite-difference solution with the analytical solution for the pressure field in a homogeneous medium with a wave velocity of 3000 m/s. Top: Source wavelet. Middle: The normalized signal at a receiver at a distance of 1500 m from the source (red: 2.5D FD, black: analytic). Bottom: absolute error of the finite-difference calculation. Here, we used $\Delta x = 12$ m and $\mu = 0.25$.

NUMERICAL EXPERIMENTS

We illustrate the 2.5D finite-difference process discussed above by means of two numerical experiments. The first tests uses a simple model, which consists of a homogeneous layer between two homogeneous half-spaces as shown in Figure 4. The velocities, from top to bottom, are 3.0 km/s, 3.5 km/s, and 4.0 km/s, respectively. For this model, we have simulated a split-spread experiment with a compressional point source located at $x = 800$ m at 24 m depth, the minimum offset is 124m. The receivers are regularly spaced around the source at intervals of 50 m at 6 m depth (see Figure 4).

The results of the 2.5D and 3D FD modeling for Model 1, for the pressure field and the vertical velocity component are presented in the Figures 5 and 6, respectively. These results were obtained by discretization on a regular grid with $\Delta x = \Delta z = 6$ m. The source is of volume injection type and the pulse is a Küpper wavelet with a dominant frequency of 14Hz.

One point to be stressed when comparing these sections is the source implementation. The source on 3D schemes are specified in a small region around the source position to avoid numerical dispersion. On the 2.5D FD, although we use a small region on the x_1x_3-plane, the source is delta function along the x_2 direction. This difference on the source specifications causes the amplitudes of 3D and 2.5D model not to match perfectly.

As the second model, we used the Marmousi velocity model (see Figure 7) to evaluate the 2.5D solution in a complex situation. The Gardner formula (Gardner et al. (1974)) was used to compute the density. The 3D model consists of part of the 2D Marmousi model from 3600 m to 9114 m discretized on a regular grid

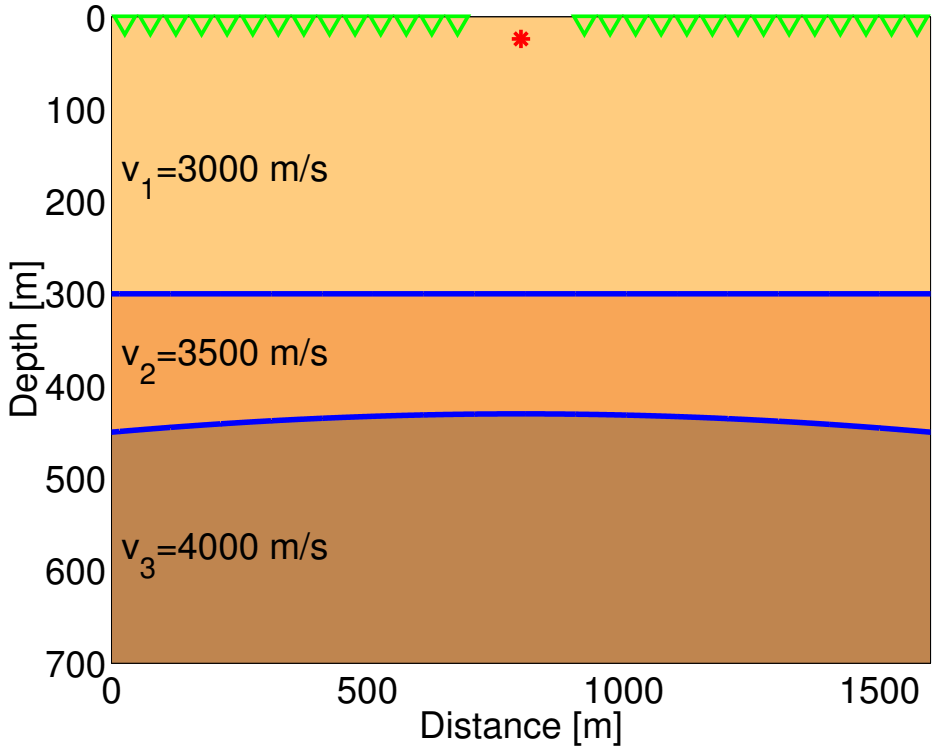

Figure 4: First model: Two interfaces separating three homogeneous layers.

with $\Delta x = 24$ m. This section was extended in the transverse direction with 120 identical panels in a 24 m interval. A free surface is assumed on the top of the model, and absorbing boundaries of the PML type (Chew and Liu, 1996) are active on the left, right and bottom of the model. The width of the absorbing layers is $20\Delta x$. For 3D and 2.5D modeling, the source is of volume injection type, located at 8000 m and 24 m depth. The pressure field is recorded by 96 receivers that are regularly spaced at every 24 m to the left of the source with 200 m minimum offset at 24 m depth. The wavelet is a Küpper pulse of 10 Hz of dominant frequency. Figure 8 compares the results of 2.5D FD to the corresponding 3D FD synthetic data. The sections show good agreement on the first 2.25 s. The differences that follow are produced in the 3D modeling by reflections on the borders in the x_2 direction which are very close to the vertical plane containing the receivers.

CONCLUSIONS

In this paper, we have extended the formulation of 2.5D acoustic finite-difference modeling to media with variable density. We have derived and discussed the stability conditions and numerical dispersion relations for high-order difference schemes. The described FD scheme allows for an immediate incorporation of absorbing boundary conditions like the ones described by Neto and Costa (2004). Moreover, we have compared the 2.5D FD modeling results with corresponding 3D results, obtaining good agreement.

Perhaps the most attractive feature of 2.5D modeling is its low memory demand. Since the method can be similarly extended to elastic case, it will become possible to compute accurate 3D wavefields in 2D models specified on a dense grid on a single PC, while the 3D approach to elastic modeling is quite demanding even for today's clusters. The generalization of this approach to viscoelastic and poroelastic media can provide a cheap approach to seismic modeling in complex exploration environments. Finally, 2.5D FD modeling can provide one more alternative to validate 3D seismic modeling codes.

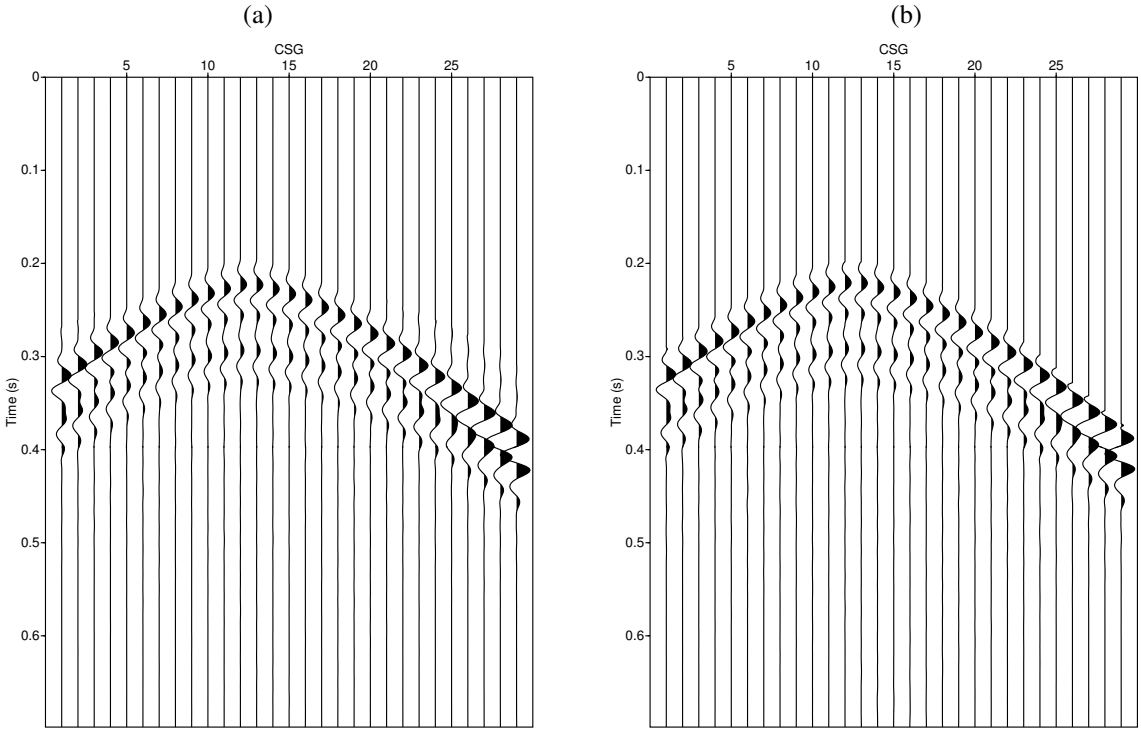

Figure 5: Pressure field for Model 1 computed using: (a) 2.5D finite difference, (b) 3D finite difference.

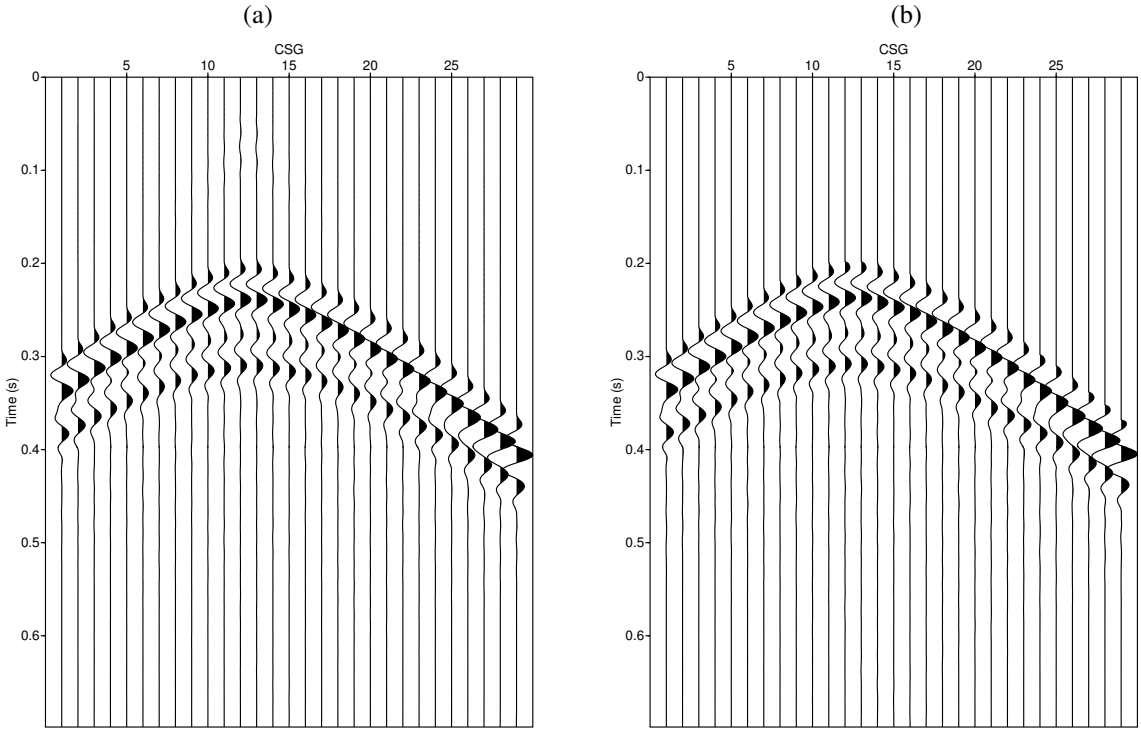

Figure 6: Vertical component of the particle velocity for Model 1, computed using: (a) 2.5D finite difference, (b) 3D finite difference.

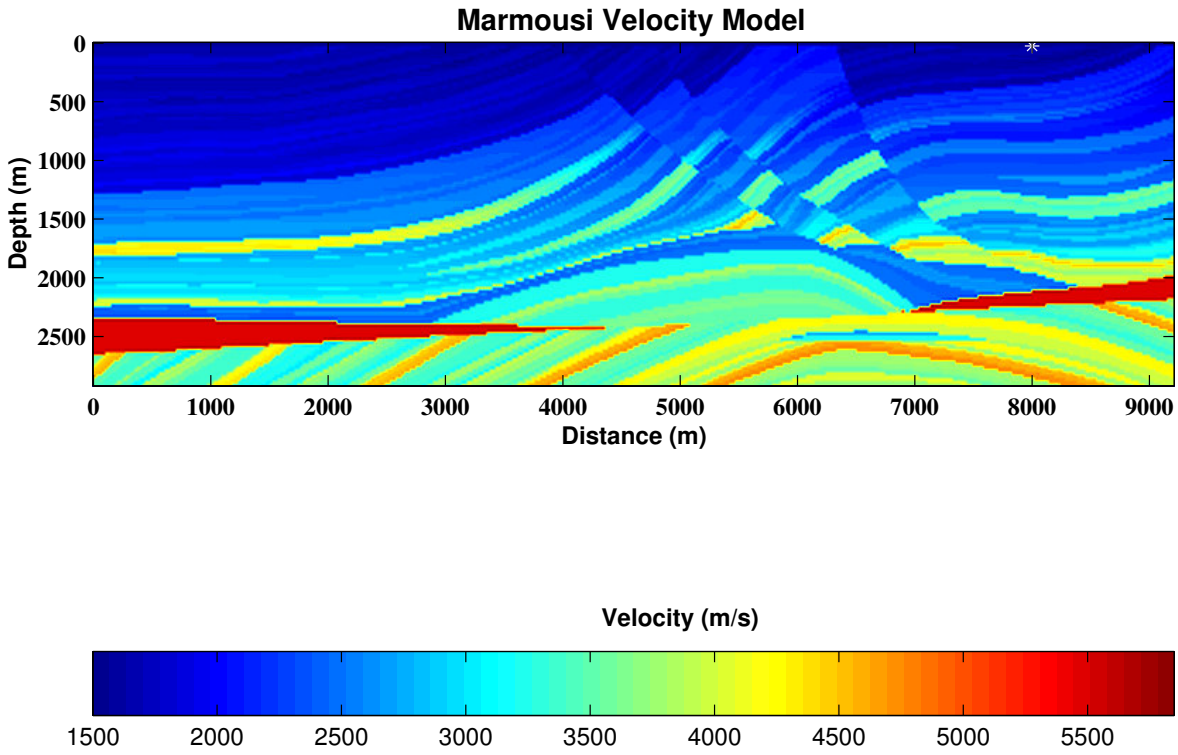

Figure 7: Second model: Marmousi model.

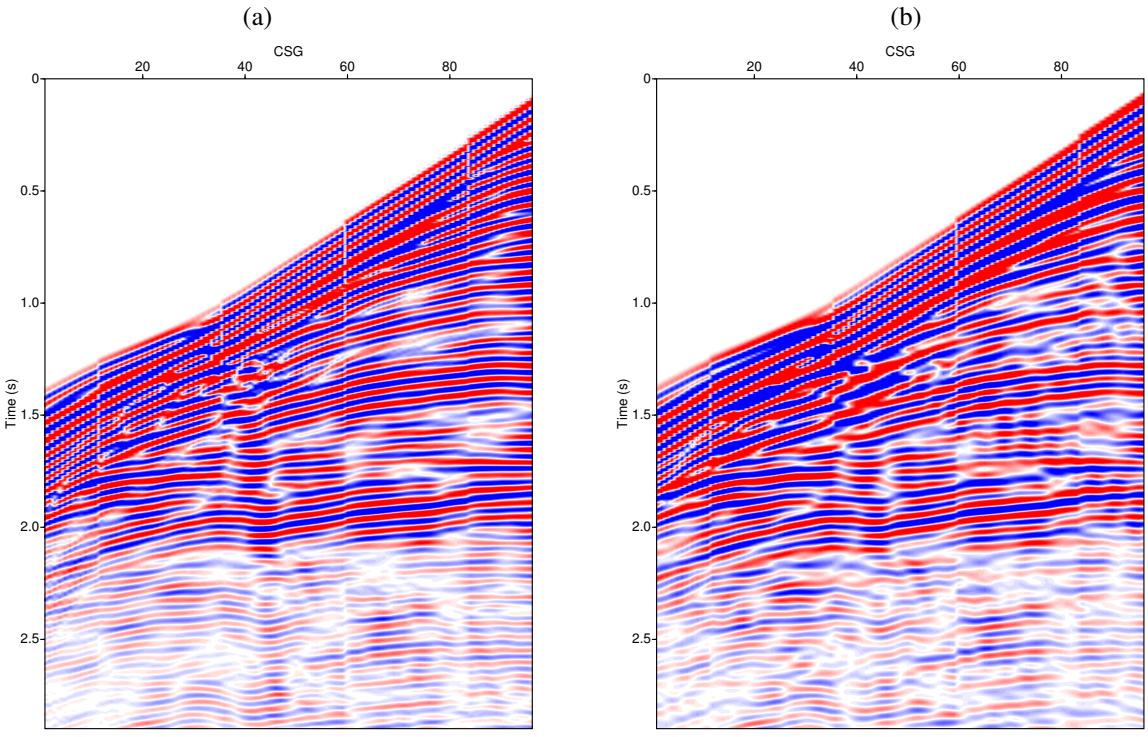

Figure 8: Marmousi model: (a) 2.5D finite difference, and (b) 3D finite difference.

ACKNOWLEDGMENTS

This work was kindly supported by CNPq, Brazil, and the sponsors of the *Wave Inversion Technology (WIT) Consortium*, Karlsruhe, Germany.

REFERENCES

Aki, K. and Richards, P. (1980). *Quantitative Seismology – Vol. 1: Theory and Methods*. W.H. Freeman, New York.

Cao, S. and Greenhalgh, S. (1998). 2.5-D modeling of seismic wave propagation: Boundary condition, stability criterion, and efficiency. *Geophysics*, 63(6):2082–2090.

Chew, W. and Liu, H. Q. (1996). Perfectly matched layers for elastodynamics: a new absorbing boundary condition. *J. Computational. Acoust.*, 4(4):341–359.

Gardner, G. H. F., Gardner, L. W., and Gregory, A. R. (1974). Formation velocity and density—the diagnostic basics for stratigraphic traps. *Geophysics*, 39(6):770–780.

Iserles, A. (1996). *A first course in the numerical analysis of differential equations*. Cambridge University Press.

Karrenbach, M. (1995). *Elastic tensor wave fields*. PhD thesis, Stanford University. URL: http://sepwww.stanford.edu/public/docs/sep83/.

Levander, A. R. (1988). Fourth-order finite-difference P-SV seismograms. *Geophysics*, 53(11):1425–1436.

Liner, C. L. (1991). Theory of a 2.5-D acoustic wave equation for constant density media. *Geophysics*, 56(12):2114–2117.

Neto, F. and Costa, J. (2004). Modelagem acústica por diferenças finitas e elementos finitos em meios geologicamente complexos. I Workshop da Rede de Risco Exploratório, Natal, RN, Brazil.

Novais, A. and Santos, L. (2004). 2.5D finite-difference solution of the acoustic wave equation. *Geophysical Prospecting in press*.

Song, Z. and Williamson, P. R. (1995). Frequency-domain acoustic-wave modeling and inversion of cross-hole data: Part I—2.5-D modeling method. *Geophysics*, 60(3):784–795.

Thomas, J. (1995). *Numerical Partial Differential Equations*. Springer-Verlag, New York.

Williamson, P. R. and Pratt, R. G. (1995). A critical review of acoustic wave modeling procedures in 2.5 dimensions. *Geophysics*, 60(2):591–595.

Zhou, B. and Greenhalgh, S. A. (1998). Composite boundary-valued solution of the 2.5-D Green's function for arbitrary acoustic media. *Geophysics*, 63(5):1813–1823.